Characteristics of Ammonia Adsorption on Activated Alumina

Dipendu Saha* and Shuguang Deng

Chemical Engineering Department, New Mexico State University, Las Cruces, New Mexico 88003, United States

Adsorption of ammonia was measured volumetrically on activated alumina at temperatures of (273, 298, and 323) K and gas pressures up to 108 kPa. It was found that the final adsorption amounts at the terminal pressure point were (3.13, 2.53, and 1.89) mmol·g^{-1} at (273, 298, and 323) K, respectively. The Langmuir, Freundlich, Sips, and Toth isotherm models were employed to correlate the adsorption isotherms. Ammonia diffusivities in these adsorbents at (298 and 323) K and at five different pressure points were calculated from the adsorption kinetic uptake curves by using a classical diffusion model. It was found that the average diffusivity values were ($4.02 \cdot 10^{-14}$ and $4.71 \cdot 10^{-14}$) m^2·s^{-1}, respectively, at (298 and 323) K. The heat of adsorption values are between (−35.6 and −15) kJ·mol^{-1} for adsorption loadings between (1.3 and 2.3) mmol·g^{-1}. The Gibbs energies were calculated as (−14.01, −13.23, and −9.07) kJ·mol^{-1} at (323, 298, and 273) K, respectively. The value of the entropy lies within (−65 to −3) J·mol^{-1}·K^{-1}, (−73 to −6) J·mol^{-1}·K^{-1}, and (−95 to −21) J·mol^{-1}·K^{-1} for adsorption amounts of (1.3 to 2.3) mmol·g^{-1} and at temperatures of (323, 298, and 273) K, respectively.

1. Introduction

Incessant deterioration of pristine environmental quality by anthropogenic activities has become a major concern in the present day. Despite being a quite important industrial gas, ammonia is one of the most threatening polluting gases that started to become an increasingly severe global problem after the beginning of industrialization.[1] It is a strong air pollutant that contributes to particulate matter formation[2] and is also highly toxic to humans because of its basicity and very high water solubility.[3] It attacks the respiratory system, skin, and eyes via an exothermic reaction leading to severe burning. A prolonged exposure at a concentration higher than 300 ppm (mg·L^{-1}) may cause irreversible damage to the body that might lead to death.[4−6]

The ammonia molecule is basic and polar in nature, and therefore, several types of surface-modified adsorbents have been utilized to examine their ammonia removal efficiencies. These widespread adsorbents include numerous carbon-based adsorbents,[7−14] zeolites,[15−20] alumina or alumina composites,[18,21,22] silica,[18] or metal−organic frameworks.[23−25] Different types of surface functional groups, such as −COOH, −Cl, −SOOH, −C═O, or −OH, were attached to the carbon surface by thermal or electrochemical deposition to enhance the ammonia adsorption.[26] Huang et al.[7] doped coconut-shell-derived activated carbon with acidic groups by five different acids, and it was reported that nitric acid-doped carbon demonstrated the best uptake capacity. Kim and Park[8] modified a porous carbon by treatment with nitric acid and reported that the sorption capacity increases with an increase in the density of surface carbonyl groups. Leuch and Bandosz[10] impregnated commercially available activated carbon with metallic salts (iron, cobalt, and chromium) to enhance the ammonia sorption capacity by reactive adsorption. Shen et al.[12] modified amylase- and amylopectin-derived carbon with nitric and sulfuric acids, and the ammonia adsorption was reported to be as high as 22 % (by weight) for sulfuric acid-treated amylase-derived carbon. Rodriguez et al.[9] performed a breakthrough study of ammonia adsorption with activated carbon without any surface modification. Ellison et al.[13] reported ammonia adsorption onto a bundle of single-wall carbon nanotubes (SWNTs). Saha and Deng[14] employed ordered mesoporous carbon (OMC) to measure the equilibrium and kinetics of ammonia adsorption at ambient temperature.

Numerous types of zeolites have been employed for ammonia adsorption studies. It is generally said that the inherent Brønsted acid groups on the surface of zeolite materials help them to capture ammonia molecules. Zeolite 13X has been widely employed by different researchers to measure the ammonia uptake at different conditions. Singh and Prasad[16] used 13X to remove the NH_4^+ ion from coke plant wastewater. Zheng et al.[17] also employed 13X to remove NH_4^+ from water and measured the thermodynamic properties such as the heat of adsorption and Gibbs energy for ammonia uptake. Helminen et al.[18] employed different commercial brands of 13X, 5A, 4A, dealuminated pentasil, faujasite, clinoptilolite, alumina, and silica to compare their ammonia adsorption efficiencies. Ducourty et al.[15] used gallium-based zeolites to measure ammonia uptake by microcalorimetry. Kapustin and Brueva[19] utilized a stepwise thermodesorption method for the rapid estimation of the heat of ammonia adsorption and number of acidic sites of zeolites A, Y, mordenite, and erionite. Nicolaides et al.[20] employed a microcalorimetric study of ammonia adsorption on ZSM-5, and it was found that the heat of adsorption was as high as (120 to 140) kJ·mol^{-1}, definitely suggesting the strong binding of ammonia with surface Brønsted acid groups.

Alumina composites with zirconium and graphitic oxide were employed by Sedych and Bandosz,[21,22] and it was found that the surface acidic groups play a vital role in attracting ammonia within the cages. A breakthrough amount of 6 mg·g^{-1} of ammonia adsorption was measured in MOF-5 by Britt et al.[23] and Petit and Bandosz;[24] however, Saha and Deng[25] reported that ammonia damages MOF-5 and MOF-177 by forming a hydrogen bond with the zinc centers of the framework.

* Corresponding author. Phone: (865) 574-0798. Fax: (865) 576-8424. E-mail: dipendus@gmail.com.

10.1021/je100405k
Published on Web 11/19/2010

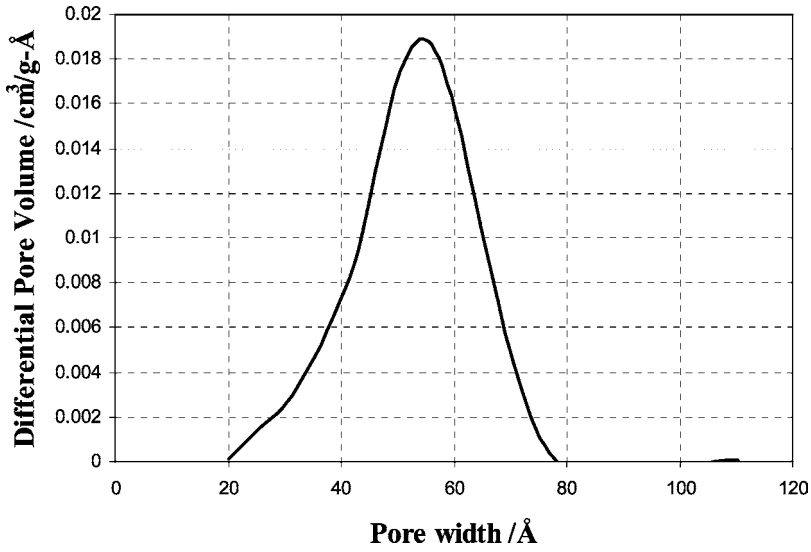

Figure 1. Pore size distribution of the activated alumina sample by the BJH method.

The objective of the present study is to measure the ammonia adsorption behavior of activated alumina synthesized by a sol−gel technique and to calculate different transport and thermodynamic properties of ammonia adsorption. Adsorption equilibria were measured at three different temperatures of (273, 298, and 323) K and pressures up to 108 kPa followed by isotherm modeling by four different equations. The kinetic data of adsorption were recorded at five different pressure levels and two temperatures [(298 and 323) K] along with the estimation of intracrystalline diffusivity at each point. Different thermodynamic properties along with the heat and entropy of adsorption and Gibbs energy were also calculated for this adsorption study. These data will provide necessary information for adsorbent selection and process design for the pressure swing adsorption (PSA) processes for ammonia separation and recovery; the thermodynamic parameters will also help us to understand adsorption fundamentals.

2. Experimental Section

2.1. Materials. Activated alumina by a sol−gel technique was synthesized according to the previously published works.[27] Commercially available highest purity ammonia (Matheson trigas) was employed for the adsorption measurement.

2.2. Adsorption Measurement. 2.2.1. N_2 Adsorption−Desorption Study. The alumina samples were characterized for their pore textural properties with nitrogen adsorption and desorption at the liquid nitrogen temperature in a Micromeritics ASAP 2020 adsorption apparatus. The pore textural properties including the Brunauer−Emmett−Teller (BET) specific surface area, pore volume, and pore size were obtained by analyzing the nitrogen adsorption and desorption isotherms with the Micromeritics ASAP 2020 built-in software. Before the nitrogen adsorption measurements were started, each sample was activated by degassing in situ at 573 K for 12 h to remove the guest molecules from the pores of the alumina samples.

2.2.2. Ammonia Adsorption Study. The equilibrium and kinetics of ammonia adsorption on both adsorbents were measured volumetrically in the same Micromeritics ASAP 2020 surface area and porosity analyzer. Adsorption isotherms were measured at three temperatures [(323, 298, and 273) K] and NH_3 pressures up to 108 kPa. The temperature of the sample bath was constantly monitored with the help of a thermocouple, and it was observed that the temperature variation was no more than ± 1 K for experiments at (298 and 323) K and ± 2 K for experiments at 273 K. The temperatures of (273, 298, and 323) K were achieved by using regular ice, room temperature water, and a heating mantle, respectively. Kinetic data were recorded during the isotherm measurements at (298 and 323) K and five different pressures. The alumina samples were activated at 573 K under a vacuum ($1.33 \cdot 10^{-6}$ kPa) for 12 h before the adsorption measurements. High-purity ammonia was introduced into a gas port of the adsorption unit for the adsorption measurements. To ensure that the instrument was measuring each data point accurately, it was calibrated by employing two standards which were provided by the instrument manufacturing company, and it was found that the measured values were within ± 2 % error with the given values. Each of the isotherms reported in this paper was repeated three times, and it was noticed that the data points varied by no more than ± 1 %.

3. Results and Discussion

3.1. Pore Texture Properties. The pore textural properties of activated alumina were calculated from the nitrogen adsorption−desorption plot by using the instrument's built-in software. The BET specific surface area of this material is 274 $m^2 \cdot g^{-1}$. The pore size distribution by using the Barret−Joyner−Halenda (BJH) method is shown in Figure 1. It is also calculated that the median pore width and cumulative pore volume of this material are 49.6 Å and 0.5 $cm^3 \cdot g^{-1}$, respectively, on the basis of the BJH method.

3.2. Adsorption Equilibrium. Adsorption isotherms of ammonia on activated alumina at (273, 298, and 323) K are given in Figure 2. It is observed that the equilibrium adsorption amounts at the terminal pressure range (∼108 kPa) are (3.13, 2.53, and 1.89) $mmol \cdot g^{-1}$ at (273, 298, and 323) K, respectively. The adsorption amounts were in a range similar to that reported by Helminen et al.[18] for different types of commercial alumina samples [(2 to 3) $mmol \cdot g^{-1}$] at 298.15 K and up to 100 kPa. The adsorption isotherms obtained in this work are modeled by employing the Langmuir, Freundlich, Sips (Langmuir−Freundlich), and Toth models. The Langmuir equation is given by

$$q = \frac{a_m bp}{1 + bp} \tag{1}$$

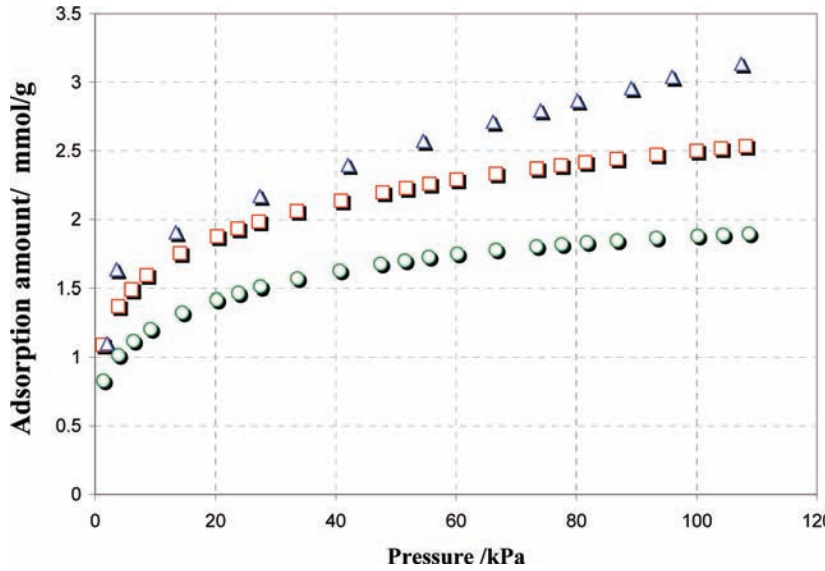

Figure 2. Adsorption isotherms of ammonia on alumina at (273, 298, and 323) K: ○, 323 K; □, 298 K; △, 273 K.

where a_m (mmol·g^{-1}) is the monolayer adsorption capacity, b (kPa^{-1}) is the Langmuir adsorption equilibrium constant, p is the pressure (kPa), and q is the adsorption amount (mmol·g^{-1}). Both the parameters can be determined from the slope and intercept of a linear plot of $1/p$ versus $1/q$.

The Freundlich model can be written as

$$q = kp^{1/n} \tag{2}$$

where k and n are the equation model parameters which can be calculated from a linear plot of ln p versus ln q.

The Sips (Langmuir−Freundlich) model can be written as

$$q = \frac{a_m b p^{1/n}}{1 + bp^{1/n}} \tag{3}$$

The Toth model can be given by

$$q = \frac{\alpha_T p}{(k_T + p^t)^{1/t}} \tag{4}$$

where α_T, k_T, and t are the equation constants. All the equation parameters of the Sips and Toth models can be calculated by nonliner regression techniques. The degree of model fitting was compared by the absolute relative error (ARE; %), calculated as

$$\text{ARE}/\% = \frac{\sum_{n=1}^{N} |x_{\text{exptl}} - x_{\text{mod}}|}{N} \cdot 100 \tag{5}$$

where x_{exptl} is the experimental point, x_{mod} is the modeling point, and N is the number of points in the isotherm.

Tables 1 summarizes the isotherm model parameters and ARE values for ammonia adsorption onto activated alumina. Figure 3 compares the model fitting with the experimental values for (273, 298, and 323) K. From the plots, it is quite obvious that the Freundlich, Toth, and Sips models fit well for all three isotherms. However, the ARE values from the table suggest that the Freundlich, Toth, and Sips models fit best at the temperatures of (273, 298, and 323) K, respectively.

Table 1. Isotherm Model Parameters

isotherm model	model param	temp / K	param value	ARE / %
Langmuir	a_m	273	2.797	20.46
	b		0.334	
	a_m	298	2.238	18.50
	b		0.652	
	a_m	323	1.702	13.80
	b		0.596	
Freundlich	k	273	0.962	5.78
	n		4.00	
	k	298	1.063	0.84
	n		5.344	
	k	323	0.791	1.57
	n		5.224	
Sips	a_m	273	16.428	6.83
	b		0.066	
	n		3.806	
	a_m	298	6.058	0.84
	b		0.201	
	n		3.700	
	a_m	323	3.889	0.93
	b		0.234	
	n		3.316	
Toth	k_T	273	0.383	6.42
	α_T		159.865	
	t		0.063	
	k_T	298	0.261	0.17
	α_T		160.105	
	t		0.046	
	k_T	323	0.265	1.17
	α_T		137.084	
	t		0.045	

3.2. Adsorption Kinetics. The adsorption kinetic data of ammonia were collected at the same time when the isotherms were generated at (298 and 323) K and pressures up to 108 kPa. Figure 4 shows the kinetic plots at five different pressure ranges at (298 and 323) K. It is observed that the adsorbent reached the adsorption saturation level within (40 to 50) s and (30 to 40) s at (298 and 323) K. A classical diffusion model was applied to analyze the kinetic data and to estimate the diffusivity of ammonia in our alumina samples. For fractional uptakes (m_t/m_∞) higher than 70 %, the diffusion model equation can be written as[28]

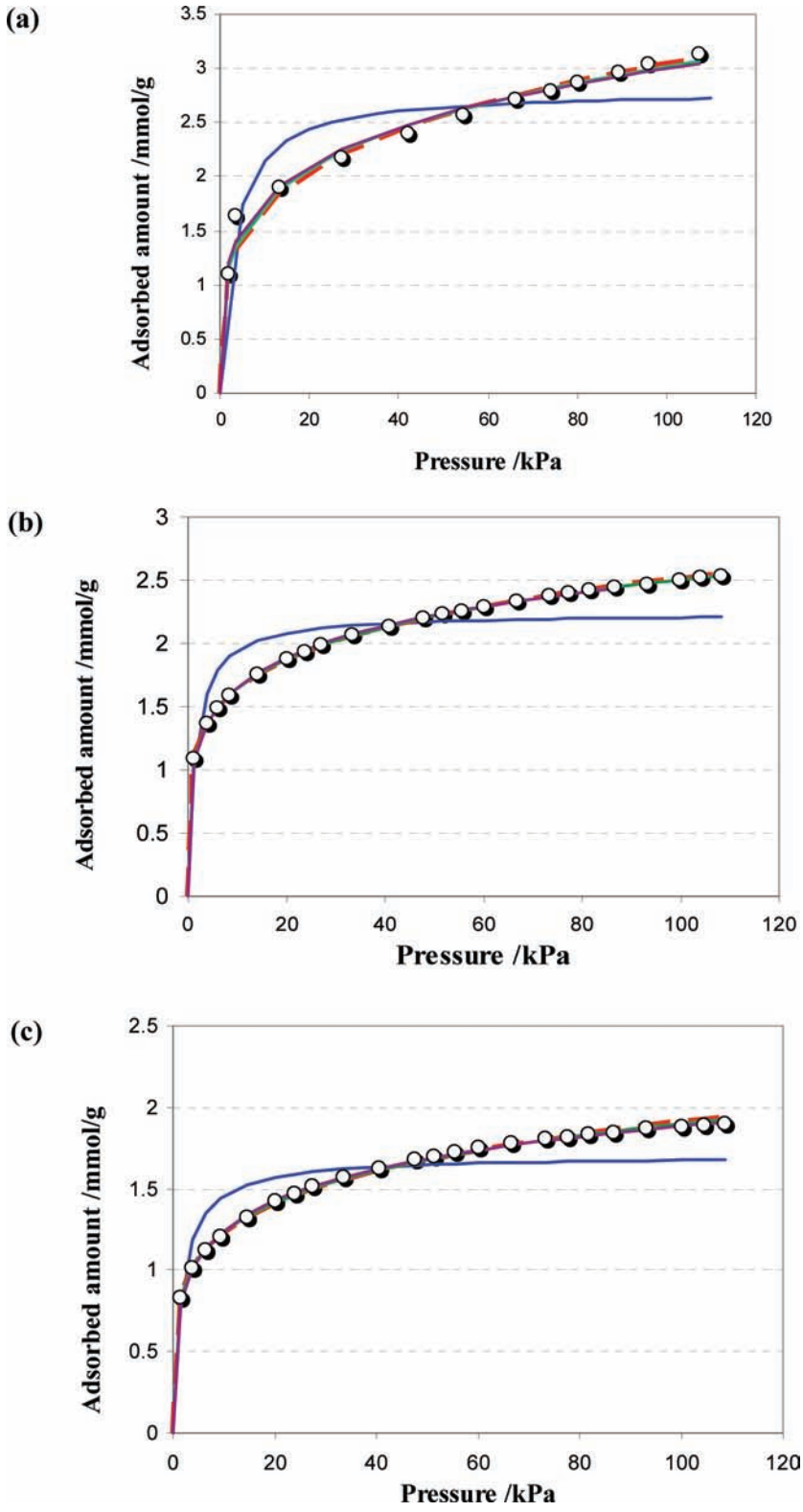

Figure 3. Isotherm model fitting at 273 K (a), 298 K (b), and 323 K (c): ○, experimental value; solid line, Langmuir model; red dashed line, Freundlich model; green solid line, Toth model; purple solid line, Sips model.

$$1 - \frac{m_t}{m_\infty} = \frac{6}{\pi^2} \exp\left(\frac{-\pi^2 D_c t}{r_c^{\,2}}\right) \qquad (6)$$

where D_c is the intracrystalline diffusivity, r_c is the equivalent crystal radius, and t is time. The diffusion time constants D_c/r_c^2 (s^{-1}) were calculated from the slope of a linear plot of $\ln(1 - m_t/m_\infty)$ versus t at a given NH_3 pressure. The errors of the linear fits of these plots were observed to vary within 0.85 to 0.95 for R^2 values. It has been found from the scanning electron microscopy (SEM) images (not reported here) that the alumina samples possess an equivalent crystalline radius of $1.0 \cdot 10^{-6}$ m. From this crystal radius size values of the average diffusivities of NH_3 are calculated to be ($4.02 \cdot 10^{-14}$ and $4.71 \cdot 10^{-14}$) $m^2 \cdot s^{-1}$ at (298 and 323) K, respectively. The variations of diffusivity with pressure are shown in Figure 5 for (298 and 323) K. It is

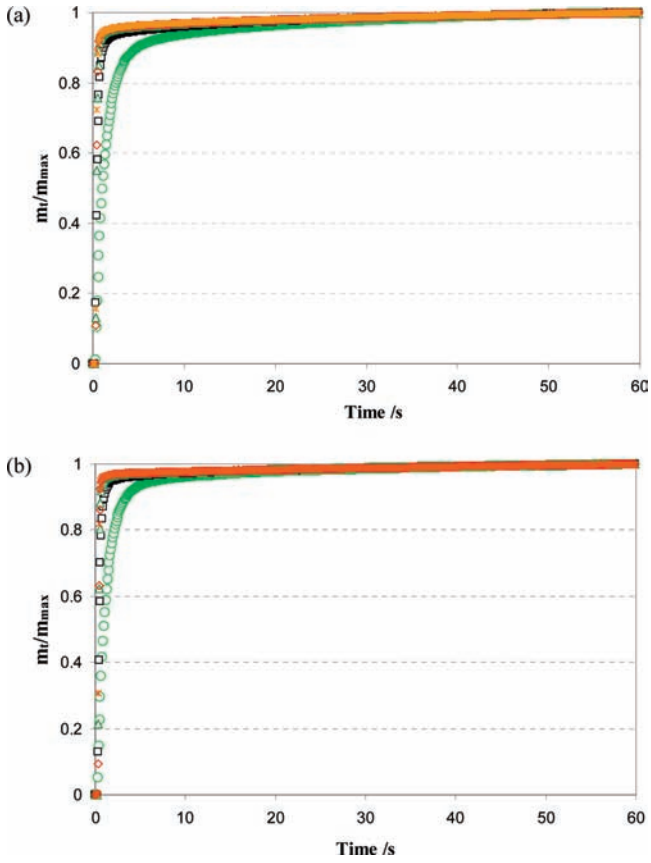

Figure 4. Kinetic plots of ammonia adsorption at 298 K (a) and 323 K (b): ○, 6.5 kPa; □, 27.6 kPa; △, 55.6 kPa; ◇, 81.7 kPa; *, 108.6 kPa.

observed that the diffusivity values decrease with increasing pressure. This trend is probably attributed to the fact that the pores of the adsorbent material are partially saturated and blocked at the higher adsorption loading at elevated pressures.

To investigate the effect of Knudsen diffusivity in the adsorption process, we calculated the Knudsen diffusivity (D_k) values. The Knudsen diffusivity can be calculated as

$$D_k = 9700r\sqrt{\frac{T}{M}} \tag{7}$$

where r is the cylindrical pore radius, T is the temperature (K), and M is the molecular weight of the diffusing species. Assuming the alumina samples contain a cylindrical pore diameter of 49.6 Å, it was found that the Knudsen diffusivity values are ($1.005 \cdot 10^{-6}$ and $1.045 \cdot 10^{-6}$) $m^2 \cdot s^{-1}$ at (298 and 323) K, respectively. As the Knudsen diffusivity values are of the order of 10^8 times larger than the molecular (intracrystalline) diffusivity values, it can be concluded that the key controlling factor of the adsorption process is the molecular diffusivity.

3.3. Activation Energy for Diffusion. The activation energy for diffusion can be calculated from the Eyring equation given by

$$\ln\left(\frac{D_c}{D_c o}\right) = \frac{-E_a}{RT} \tag{8}$$

where E_a is the activation energy, which can be calculated from the slope of the plot of $\ln(D_c)$ versus $1/T$. It was found that the activation energy was 5.07 $kJ \cdot mol^{-1}$, which is similar to the activation energies calculated for hydrocarbon adsorption onto zeolite materials.[28]

3.3. Thermodynamic Parameters. 3.3.1. Heat of Adsorption. The isosteric heat of adsorption values are a quite important parameter revealing the adsorbate−adsorbent interactions. The isosteric heat of adsorption can be calculated from the van't Hoff equation

$$\frac{\Delta H}{RT^2} = -\left(\frac{\partial \ln P}{\partial T}\right)_q \tag{9}$$

where ΔH is the isosteric heat of adsorption ($kJ \cdot mol^{-1}$), P is the gas pressure (kPa), T is the temperature, and q is the adsorption amount ($mmol \cdot g^{-1}$). Integration of eq 9 yields

$$\ln P = \frac{\Delta H}{RT} + C \tag{10}$$

where C is an integration constant. In this work, the isotherms at (273, 298, and 323) K were employed to calculate the heat of adsorption values. The isotherm data points were first converted to a set of isosteres (linear plot of ln P versus $1/T$)

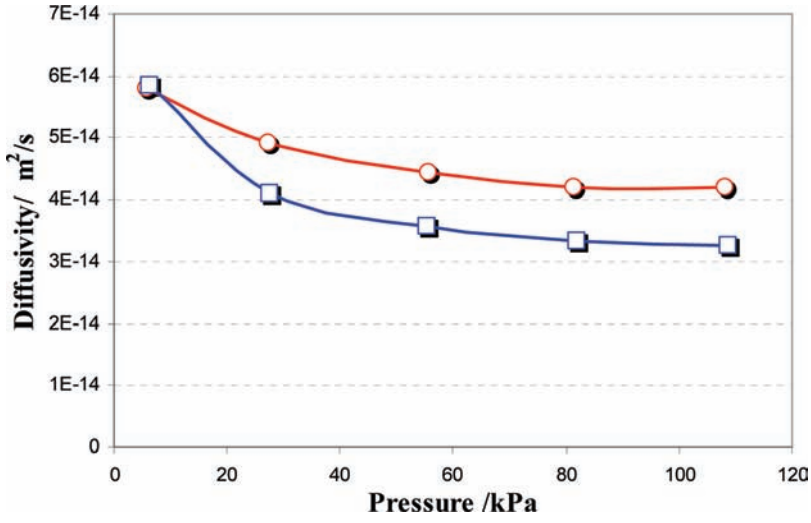

Figure 5. Variation of the ammonia diffusivity with pressure: ○, 323 K; □, 298 K.

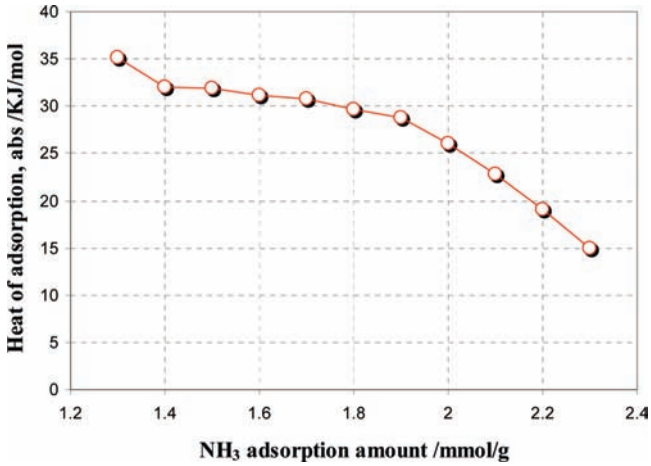

Figure 6. Heat of adsorption of ammonia.

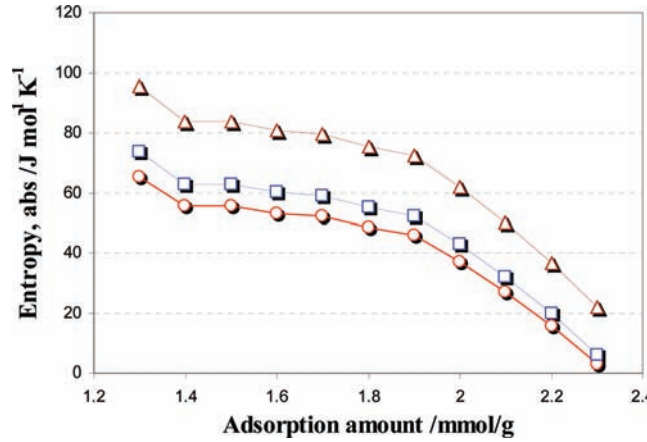

Figure 7. Entropy of the adsorption of ammonia: ○, 323 K; □, 298 K; △, 273 K.

and then correlated with eq 10 followed by calculation of the heat of adsorption from the slope of the isosteres according to eq 10. The variation of the heat of adsorption with the adsorption loading is plotted in Figure 6. It is observed that these values were (−35.6 to −15) kJ·mol^{-1} within an adsorption loading of (1.3 to 2.3) mmol·g^{-1}. The higher sides of the heat of adsorption values are significantly lower than that reported for surface-modified carbon or zeolites. The molar heat of adsorption was reported to be (−150 to −50) kJ·mol^{-1} up to 150 μmol·g^{-1} for surface-modified commercial activated carbons.[11] The heat of adsorption was also as high as (140 to 150) kJ·mol^{-1} within the same adsorption loading for Ga-MFI and ZSM-5 zeolites.[15,20] The quite lower values of the heat of adsorption for activated alumina suggest that the interaction between ammonia and activated alumina is quite weak and the chemical binding between these two species is quite unlikely.

3.3.2. Gibbs Energy. The Gibbs energy (ΔG) is a measure of the spontaneity of a system undergoing any process. The adsorptive Gibbs energy (ΔG) can be written as

$$\Delta G = -nRT \tag{11}$$

where n is the equilibrium adsorption coefficient. As the Freundlich model fits quite well for all the isotherms, n can be correlated to the model parameter of the Freundlich equation. With the help of eq 9, the ΔG values for ammonia adsorption can be calculated as (−14.01, −13.23, and −9.07) kJ·mol^{-1} at (323, 298, and 273) K, respectively. The absolute values of ΔG were lower than that reported for NH_4^+ adsorption [(3.7 to 5.1) kJ·mol^{-1}] by Zheng et al.[17] It is also noticeable that the change in Gibbs energy is negative for all the cases, suggesting the spontaneity of the process.

3.3.3. Entropy. The entropy (ΔS) can be calculated from the Gibbs−Helmohltz equation given by

$$\Delta G = \Delta H - T\Delta S \tag{12}$$

The entropy values were calculated from each value of enthalpy at different adsorption amounts and three distinct temperatures of (323, 298, and 323) K and are shown in Figure 7. It is observed that the entropy values are all negative and decrease with increasing adsorption amount. The value of entropy lies within (−65 to −3) J·mol^{-1}·K^{-1}, (−73 to −6) J·mol^{-1}·K^{-1}, and (−95 to −21) J·mol^{-1}·K^{-1} for an adsorption amount of (1.3 to 2.3) mmol·g^{-1} and at temperatures of (323, 298, and 273) K, respectively. The absolute values of the higher ends of entropy are lower than the entropy of NH_4^+ adsorption (−72.9 J·mol^{-1}·K^{-1}) calculated by Zheng et al.[17] It is also worth mentioning that the absolute value of entropy increases with a decrease in temperature, suggesting that the adsorption process is more spontaneous at lower temperature.

4. Conclusion

Ammonia adsorption experiments were performed on activated alumina at three distinct temperatures and pressures up to 108 kPa, and it was found that the equilibrium adsorption amounts were (3.13, 2.53, and 1.89) mmol·g^{-1} at (273, 298, and 323) K and at the terminal pressure point. All isotherms were modeled by the Langmuir, Freundlich, Sips, and Toth models, and it was found that the Freundlich, Sips, and Toth models fit well for almost all of the isotherms. A kinetic study revealed that the average diffusivity of NH_3 was ($4.02 \cdot 10^{-14}$ and $4.71 \cdot 10^{-14}$) m^2·s^{-1} at (298 and 273) K, respectively. The diffusivity values decrease with partial pressure, which is probably attributed to the partial pore blocking at the greater adsorption amount at higher pressures. The heat of adsorption values were calculated to be (−35.6 to −15) kJ·mol^{-1} within an adsorption loading of (1.6 to 2.3) mmol·g^{-1}. The Gibbs energy was calculated as (−14.01, −13.23, and −9.07) kJ·mol^{-1} at (323, 298, and 273) K, respectively. The entropy of adsorption was calculated to be negative and decreases with increasing adsorption amount and temperature.

Acknowledgment

We acknowledge Dr. Lucy M. Camacho for synthesizing and providing the activated alumina samples.

Literature Cited

(1) Bretschneider, B.; Kurfurst, J. *Air Pollution Control Technology*; Publishers of Technical Literature: Prague, Czech Republic, 1987.
(2) Manahan., S. E. *Environmental Chemistry*, 7th ed.; Lewis: Boca Raton, FL, 1999.
(3) Petit, C.; Bandosz, T. J. Activated carbons modified with aluminium−zirconium polycations as adsorbents for ammonia. *Microporous Mesoporous Mater.* **2008**, *114*, 137–147.
(4) Netting, J. North Carolina reflects on ammonia controls. *Nature* **2008**, *406*, 928–928.
(5) Calvert, S.; Englund, H. M. *Handbook of Air Pollution Technology*; Wiley: New York, 1984.
(6) Bansal, R. C.; Goyal, M. *Activated Carbon Adsorption*; Taylor and Francis: Boca Raton, FL, 2005.
(7) Huang, C. C.; Li., H.-S.; Chen, C. H. Effect of surface acidic oxides of activated carbon on adsorption of ammonia. *J. Hazardous Mater.* **2008**, *159*, 523–527.

(8) Kim, B. J.; Park, S. J. Effects of carbonyl group formation on ammonia adsorption of porous carbon surfaces. *J. Colloid Interface Sci.* **2007**, *311*, 311–314.

(9) Rodrigues, C. C.; Moraes, D., Jr.; No'brega, S. W.; Barboza, M. G. Ammonia adsorption in a fixed bed of activated carbon. *Bioresour. Technol.* **2007**, *98*, 886–891.

(10) Leuch, L. M.; Bandosz, T. J. The role of water and surface acidity on the reactive adsorption of ammonia on modified activated carbons. *Carbon* **2007**, *45*, 568–578.

(11) Garcıa, M. D.; Groszek, A. D.; López-Garzón, F. J.; Pérez-Mendoza, M. Dynamic adsorption of ammonia on activated carbons measured by flow microcalorimetry. *Appl. Catal. A* **2002**, *233*, 141–150.

(12) Shen, W.; Zhanga, S.; Jiang, P.; Liu, Y. Surface chemistry of pyrolyzed starch carbons on adsorption of ammonia and carbon disulfide. *Colloids Surf., A* **2010**, *356*, 16–20.

(13) Ellison, M. D.; Crotty, M. J.; Koh, D.; Spray, R. L.; Tate, K. E. Adsorption of NH_3 and NO_2 on single-walled carbon nanotubes. *J. Phys. Chem. B* **2004**, *108*, 7938–7943.

(14) Saha, D.; Deng, S. Adsorption equilibrium and kinetics of CO_2, CH_4, N_2O, and NH_3 on ordered mesoporous carbon. *J. Colloid Interface Sci.* **2010**, *345*, 402–409.

(15) Ducourty, B.; Occellib, M. L.; Auroux, A. Processes of ammonia adsorption in gallium zeolites as studied by microcalorimetry. *Thermochim. Acta* **1998**, *312*, 27–32.

(16) Singh, G.; Prasad, B. Removal of ammonia from coke-plant waste water by using synthetic zeolites. *Water Environ. Res.* **1997**, *69*, 157–161.

(17) Zheng, H.; Han, L.; Ma, H.; Zheng, Y.; Zhang, H.; Liu, D.; Liang, S. Adsorption characteristics of ammonium ion by zeolite 13X. *J. Hazardous Mater.* **2008**, *158*, 577–584.

(18) Helminen, J.; Helenius, J.; Paatero, E. Adsorption equilibria of ammonia gas on inorganic and organic sorbents at 298.15 K. *J. Chem. Eng. Data* **2001**, *46*, 391–399.

(19) Kapustin, G. I.; Brueva, T. R. A simple method for determination of heats of ammonia adsorption on catalysis from thermodesorption data. *Thermochim. Acta* **2001**, *379*, 71–75.

(20) Nicolaides, C. P.; Kung, H. H.; Makgoba, N. P.; Sincadu, N. P.; Scurrell, M. S. Characterization by ammonia adsorption microcalorimetry of substantially amorphous or partially crystalline ZSM-5 materials and correlation with catalytic activity. *Appl. Catal. A* **2002**, *223*, 29–33.

(21) Seredych, M.; Bandosz, T. J. Adsorption of ammonia on graphite oxide/aluminium polycation and graphite oxide/zirconium−aluminium polyoxycation composites. *J. Colloid Interface Sci.* **2008**, *324*, 25–35.

(22) Seredych, M.; Bandosz, T. J. Adsorption of ammonia on graphite oxide/Al13 composites. *Colloids Surf., A* **2010**, *353*, 30–36.

(23) Britt, D.; Tranchemontagne, D.; Yaghi, O. M. Metal−organic frameworks with high capacity and selectivity for harmful gases. *Proc. Natl. Acad. Sci. U.S.A.* **2008**, *105*, 11623–11627.

(24) Petit, C. C.; Bandosz, T. J. Enhanced adsorption of ammonia on metal−organic framework/graphite oxide composites: Analysis of surface interactions. *Adv. Funct. Mater.* **2010**, *20*, 111–118.

(25) Saha, D.; Deng, S. Ammonia adsorption and effects on framework stability of MOF-5 and MOF-177. *J. Colloid Interface Sci.*, submitted for publication.

(26) Bansal, R. C.; Goyal, M. *Activated Carbon Adsorption*; Taylor and Francis: Boca Raton, FL, 2005.

(27) Deng, S.; Lin, Y. S. Granulation of sol−gel-derived nanostructured alumina. *AIChE J.* **1997**, *43*, 505–514.

(28) Ruthven, D. M. *Principles of Adsorption and Adsorption Processes*; Wiley Interscience: New York, 1984.

Received for review April 22, 2010. Accepted November 6, 2010. D.S. acknowledges the Bruce Wilson scholarship provided by the Chemical Engineering Department of New Mexico State University.

JE100405K